Electronic structure and ferromagnetism in the martensitic-transformation material Ni_2FeGa

Z. H. Liu, H. N. Hu, G. D. Liu, Y. T. Cui, M. Zhang, J. L. Chen, and G. H. Wu*
State Key Laboratory of Magnetism, Institute of Physics, Chinese Academy of Sciences, P.O. Box 603, Beijing 100080, People's Republic of China

Gang Xiao
Department of Physics, Brown University, Providence, Rhode Island 02912, USA
(Received 23 July 2003; revised manuscript received 14 November 2003; published 12 April 2004)

We calculated the electronic structures of the Heusler alloy Ni_2FeGa for both the cubic and the orthorhombic structures by self-consistent full-potential linearized-augmented plane-wave method. The localized moment of Fe atom is interpreted based on the electronic structure and the popular explanation of the localized moment of Mn in Heusler alloy X_2MnY. Comparing the density of states of cubic and orthorhombic structures, we observed that a Ni peak near the density of states of *d* band for the cubic structure splits for the orthorhombic structure, indicating a band Jahn-Teller mechanism should be responsible for the structural transition. Accompanied by this transformation, an increase of Ni moment and magnetization redistribution occurred. Temperature-dependence anisotropy field shows an evidence of martensitic transformation between 125 and 190 K. The magnetic behavior seems to contain a transition from Heisenberg-like at temperature below 70 K to itinerant magnetism at temperature higher than 160 K upon martensitic transformation. Temperature dependence of saturation magnetization reveals the spontaneous magnetization at martensite and parent phase are $3.170\mu_B$ and $3.035\mu_B$, respectively. The calculated magnetic moment at martensite is $3.171\mu_B$, which is quite consistent with the experimental value. The magnetic moment of Fe and Ni atom in Heusler alloy Ni_2FeGa is analyzed based on the computational results and the experimental magnetization curves. It is found that the magnetic moment of Fe atoms is about 10–43% larger than that of α-Fe.

DOI: 10.1103/PhysRevB.69.134415 PACS number(s): 75.50.Cc, 71.20.Lp, 64.70.Kb

Heusler alloys have attracted much attention ever since the discovery by Heusler that some alloys of copper-manganese bronze and *B* subgroup elements were ferromagnetic although the constituents were themselves nonferromagnetic.[1] The stoichiometric composition of Heusler alloy is X_2YZ (space group: $Fm\bar{3}m$); usually, *XY* are transition metals or noble metals and *Z* is an *sp* element. Of these, the most studied system is Mn-based Heusler alloy in which the magnetic moment is confined to Mn atoms occupying the *Y* position.[2–4] From electronic structure calculations, it was concluded that the $3d$ electrons are well localized on the Mn atoms and the interactions are long range, extending to more than eight neighbors. The separation of the Mn ions (>4 Å) is too large for direct *d*-*d* coupling.[5] Thus, the magnetic interaction is thought to arise from an indirect interaction that takes place by means of the polarization of the conduction electrons. However, there are comparatively few studies of electronic structure and magnetic properties of Heusler alloy Ni_2FeZ. In this work, we report on these properties of the Heusler alloy Ni_2FeGa.[6,7]

As reported in our previous paper a high chemical ordering structure $L2_1$, i.e., the Heusler alloy phase, can be synthesized with Ni_2FeGa composition.[6] However, the conventional method failed in synthesizing Ni_2FeGa $L2_1$ structure, because there is a strong competition between forming γ solid solution phase and intermetallic phase during the solidification process. On the other hand adoption of the melt-spun ribbon technique can avoid γ solid solution phase and directly form the pure $L2_1$ phase. Therefore, melt-spun ribbons were used in this work.

According to the results of electronic structure calculation, a simple physical explanation of the Fe moment will be given based on the Kübler model that was used to interpret the localized character of Mn magnetization in mostly Heusler alloy X_2MnY.[5] Based on the electronic structure computed for the cubic parent phase and the orthorhombic martensite and the experimental results, the change of magnetic moment through the phase transition and the temperature dependence of magnetization are discussed in detail. It has been suggested that the structural transition is driven by a band Jahn-Teller effect that is also responsible for the redistribution of the moment between Ni and Fe atoms across martensitic transformation.

Heusler alloy Ni_2FeGa undergoes a martensitic transition from cubic $L2_1$ to orthorhombic structure upon cooling. Therefore, we calculated the electronic structure and magnetic moment of Ni_2FeGa alloy for both cubic and orthorhombic structures by self-consistent full-potential linearized-augmented plane-wave (LAPW) method based on the local spin-density approximation within the density-functional theory,[8,9] where the potential and/or the charge density in the crystal are treated with no shape approximation. The cubic structure with the space group O_h has 16 atoms in the unit cell [see Fig. 1(a)]. This is a close-packed complex cubic structure with Ni atoms at $(\frac{1}{4}\ \frac{1}{4}\ \frac{1}{4})$ and $(\frac{3}{4}\ \frac{3}{4}\ \frac{3}{4})$, Fe at (000), and Ga at $(\frac{1}{2}\ \frac{1}{2}\ \frac{1}{2})$. The lattice constant of 5.7405 Å was taken from experimental data.[6] The orthorhombic structure has the space group D_{2h}. The direction $[010]_{orth}$ of the supercell corresponds to the direction $[110]_{cubic}$ of the cubic structure. The supercell of ortho-

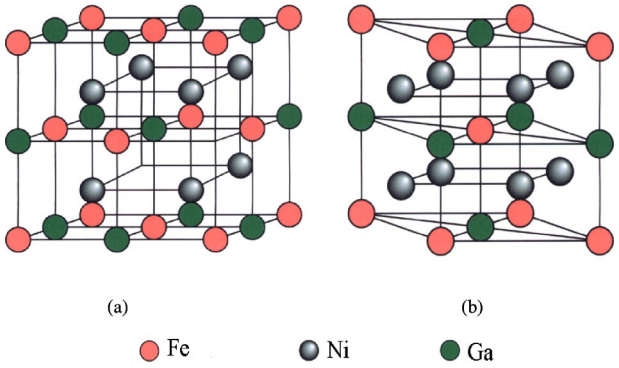

FIG. 1. Unit cells of the Ni_2FeGa (a) cubic $L2_1$ structure; (b) tetragonal structure cell in the [110] direction.

rhombic structure can be considered to consist of five tetragonal structure cells [the tetragonal structure cell is shown in Fig. 1(b)]. The experimental lattice constants, $a=5.8565$ Å, $b=5.7336$ Å, and $c=5.4507$ Å (Ref. 6) are used to calculate the electronic structure of orthorhombic structure.

The muffin-tin sphere radii R used are 2.2 a.u. for Ni, Fe and 2.3 a.u. for Ga atoms. Inside the atomic spheres the charge density and the potential are expanded in crystal harmonics up to $l=6$. The radial basis functions for each LAPW are calculated up to $l=8$ and the nonspherical potential contribution to the Hamilton matrix has an upper limit of $l=4$. The self-consistency was achieved at 60 k point for the cubic structure and 95 k point for the orthorhombic structure in the first irreducible Brillouin zone. The density plane-wave cutoff is $RK_{max}=8.0$. The electron states were treated in a scalar relativistic approximation. Using the energy eigenvalues and eigenvectors at these points, the density of states was determined by the tetrahedral integration method.[10]

The fabrication process of the samples has been published elsewhere.[6] All magnetic measurements were performed using a quantum design magnetic property measurement system.

Figure 2 shows the calculated density of state (DOS) results for the ferromagnetic state of Ni_2FeGa ribbon with cubic $L2_1$ structure. One rather strong major peak of Ga atom at about 15.48 eV below the Fermi energy is omitted from plotting the DOS graph, because it is symmetric for up-spin and down-spin states, and contributing little to the magnetism. We can see that electron states from Ni and Fe are found to have the largest contributions to the DOS. For the majority-spin states, the DOS of Ni is larger than that of Fe near the Fermi level and there are two major peaks below the Fermi level. In the minority-spin states, the Fermi level lies within the second major peak. In order to see the situation more clearly, the PDOS of d component of Ni and Fe for both spin electrons are shown in Fig. 3. Comparing with Fig. 2, it is obvious that the total DOS is mainly the decomposed d component. For the majority-spin states, the high-density region of Ni and Fe is situated in the lower energy region below the Fermi level. The Fe spin-up d state are almost completely occupied and the bandwidth indicates that it is just as delocalized as the d state of Ni. For the minority-spin states, the d bands of Ni are almost occupied and the d electrons of Fe are partially excluded from the Fe site. The Fermi level situates in a little relative high-density region of Fe d state. The Ni $3d$ state has almost equal contributions in valence band for the majority and minority spins, therefore, the mainly magnetic carrier in the Heusler alloy N_2FeGa is Fe atom.

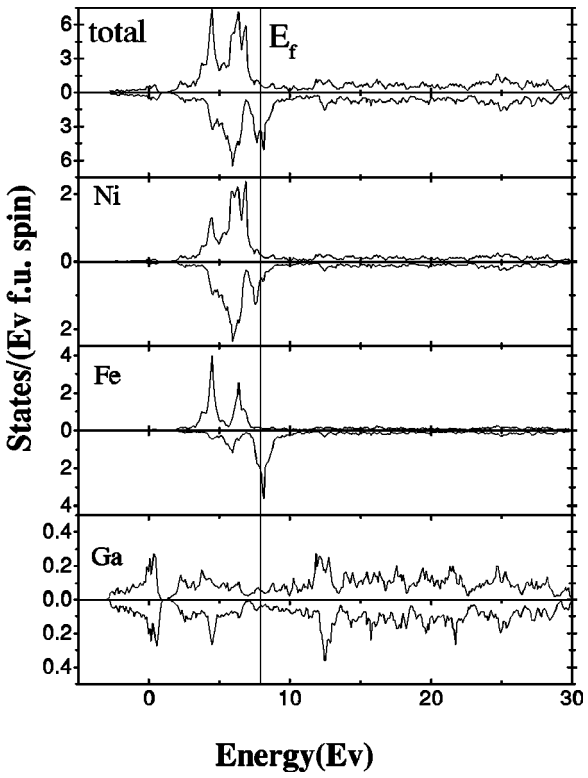

FIG. 2. Calculated spin-projected total DOS plots for cubic Ni_2FeGa. (a) The total DOS of Ni_2FeGa, (b) the total DOS of Ni atoms, (c) the total DOS of Fe atoms, (d) the total DOS of Ga atoms.

From precise electronic structure calculations and analysis for a series of Heusler alloy, Kübler *et al.* have concluded that the localized character of the magnetization in X_2MnZ alloys results from the exclusion of minority-spin electrons

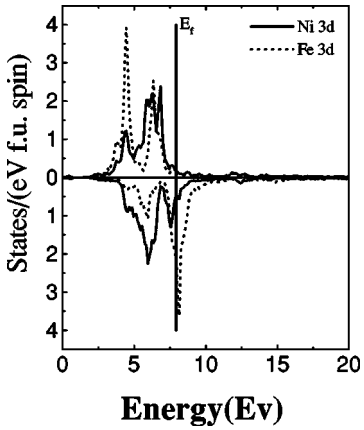

FIG. 3. The partial DOS of d component of the Ni and Fe for both spin electrons of the cubic structure. The solid line, the Ni $3d$ orbitals; the dotted line, the Fe $3d$ orbitals.

from the Mn $3d$ shell.[5] The spin-down electrons of Fe atoms in Ni_2FeGa are mostly pushed above the Fermi energy, as shown in Fig. 2. Therefore, as Kübler interpreted the electron structure for X_2MnZ, it may be reasonable to consider that this kind of localized exclusion is an equally localized region of magnetization. Thus, it can be understood that, in our case, the Fe atoms possess localized magnetic moment composed of itinerant electrons. Put differently, comparing with the DOS of Ni_2MnGa (Ref. 11) and ours, we easily detect that the spin-down electrons in Ni_2FeGa are excluded from the small region of $3d$ shell of Fe atoms not so completely as that of Mn atoms, which can be attributed to that the exchange splitting of Fe d states is not so strong as that of Mn atoms in this kind of alloys.

From Fig. 2, one can see that the major peaks in the majority-spin states are below the Fermi level. In the minority-spin states, the Fermi level is situated in the ''antibonding region.'' It implies that, as was described in the paper dealing with the band structure of Ni_3Mn,[12] the Heusler alloy Ni_2FeGa is favorable to form in disordered state. This theoretical prediction is consistent with our experiments. As we reported previously,[6] the pure ordered $L2_1$ Heusler phase of Ni_2FeGa cannot be easily synthesized as most of Heusler alloys. A nonequilibrium solidifying method, melt spinning[6] or quenching[7] from high temperature following arc melting, had to be utilized to obtain a pure $L2_1$ ordering phase. The similar situation has also been confirmed in recent works for preparing Heusler alloys Cu_2FeAl,[13] NiFeSb.[14] Their band calculation, without any exception, indicated that their Fermi levels all lie in the antibonding levels, instead of falling in the deep valley of DOS as showed by Ni_2MnGa and the others which are prepared easily by the conventional method.

The Heusler alloy Ni_2FeGa melt-spun ribbon undergoes a martensitic transformation from the cubic to the orthorhombic structures in the ferromagnetic state, so we also calculated the DOS of the orthorhombic structures. Figure 4 shows the PDOS of d component of Ni and Fe for both spin electrons. In contrast to Fig. 3, we can see that the DOS of Fe near the Fermi level are rather similar in both structures, while those of Ni are different in both structures. The DOS of Ni occurs a little split in the orthorhombic structure, which has not been observed in the cubic structure.

The total energy of a pure ferromagnetic cubic and orthorhombic structure at the experimental lattice constants is also obtained. The total energy of cubic structure is 0.59 eV/cell, higher than the value of orthorhombic structure, 0.57 eV/cell. (We take the total energy of paramagnetic phase as reference point.) It illuminated that the metastable cubic $L2_1$ phase could be stabilized by orthorhombic distortion in view of energy.

Concurrently, a magnetic moment change between the two states has been found. The calculated magnetic moments per formula unit for cubic and orthorhombic (martensite) structures are $3.126\mu_B$ and $3.171\mu_B$, respectively. For the cubic structure, the individual moment of Ni, Fe, and Ga are $0.237\mu_B$, $2.673\mu_B$, and $-0.021\mu_B$, respectively. For the martensitic structure, however, they are $0.271\mu_B$, $2.652\mu_B$, and $-0.023\mu_B$, respectively. At martensite, we will see below that the calculated total moment, μ_{total}, $3.171\mu_B$, is quite consistent with the experimental value. Also, our calculation predicts two kinds of important magnetism that the Fe atom, contributing a localized moment to Ni_2FeGa alloy, has a large magnetic moment value and the moment of Ni atom increases upon the martensitic transformation.

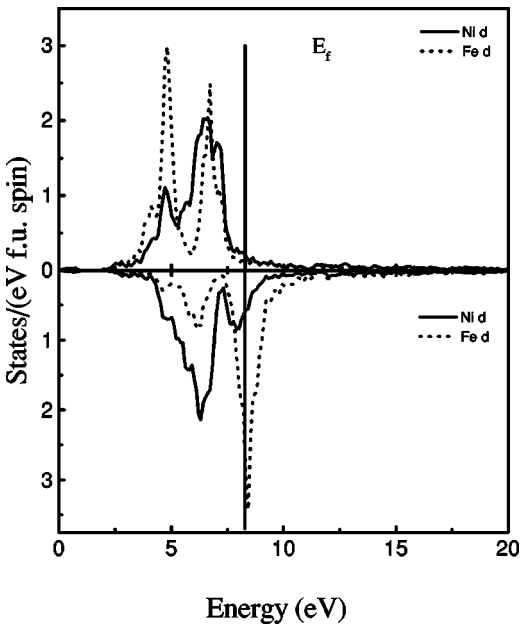

FIG. 4. The partial DOS of d component of the Ni and Fe for both spin electrons of the orthorhombic structure. The solid line, the Ni $3d$ orbitals; the dotted line, the Fe $3d$ orbitals.

From above discussion, we notice that the major DOS difference between the cubic and the orthorhombic structure is that Ni has a peak near the Fermi level for the cubic structure split for the orthorhombic one. It is worth noting that this peak split and moment transfer behaviors are very similar to those found in the Heusler alloy Ni_2MnGa.[11] It was considered that the splitting behavior plays an important role to the cubic $\rightarrow$orthorhombic structural transition. Therefore, a band Jahn-Teller effect was expected in this transition. This supposition is confirmed by spin-polarization neutron scattering experimental results of Brown *et al.*[15] Analogous to Ni_2MnGa, we think the structural transition in Ni_2FeGa is also due to the same mechanism, namely, band Jahn-Teller effect. The magnetic moment of Ni increasing across the cubic to orthorhombic structural transition is probably arising from transfer of electrons from the nearly full $3d$ band of Ni to a more than half filled $3d$ band of Fe. When the martensitic transformation occurs, the degenerate energy in the high-temperature phase splits in the low temperature, which enables the electrons to redistribute themselves so as to lower the free energy. The minority-spin Ni e_g band is lowered in the cubic to orthorhombic transition, whereas there is no significant change in the Fe bands near the Fermi surface. One can see that our calculation clearly reflected this physical mechanism.

Figure 5 shows the isothermal M-H curves measured above and below martensitic transformation. The apparent difference between the two phases is clearly seen indicating

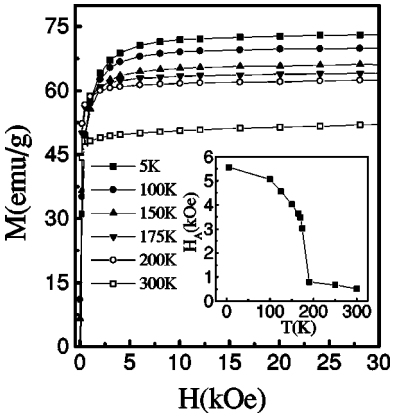

FIG. 5. Magnetization as a function of magnetic field for Ni_2FeGa ribbons at various temperatures. Inset graph shows the temperature dependence of anisotropy field.

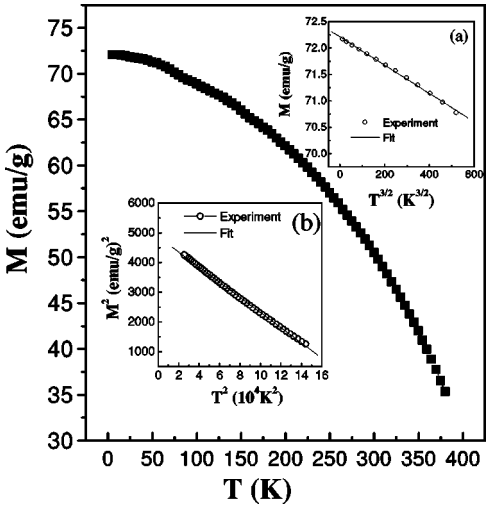

FIG. 6. Saturation magnetization as a function of temperature for Ni_2FeGa ribbons was measured over the range 5–350 K. Inset graph (a) shows the ribbon data M as a function of $T^{3/2}$ for $T<70$ K. The solid line in the inset graph is a linear fit to the Ni_2FeGa data, demonstrating the $T^{3/2}$ dependence of the magnetization for this low-T range. Inset graph (b) shows the ribbon data of M^2 as a function of T^2 for $T>160$ K. The solid line in the inset graph is a linear fit to the Ni_2FeGa data, demonstrating the T^2 dependence of M^2 for this high-T range.

a reorientation of the magnetic moment. The martensitic phase at lower temperature (at 5 K) exhibited a high-saturated magnetization of $3.170\mu_B$ and a high-anisotropy field of 0.6 T, but both decreased to $2.302\mu_B$ and 0.03 T at 300 K. The dramatic change in saturation field is attributed to the structural transition. Inset in Fig. 5 shows the temperature dependence of the anisotropy fields of Ni_2FeGa. One can see that the value of anisotropy field H_A is very small in the soft cubic phase, being of 0.078 T up to the martensitic transformation where there is a large jump taking place. Subsequently, at the martensite phase the values of H_A increase with decreasing temperature. Thus, we can infer from this plot that the martensitic transformation occurs between 125 K and 190 K. This transformation behavior is consistent with the above result that total energy is favorable for the orthorhombic distortion. For the martensite saturation magnetization at 5 K, one can see that the experimental value, $3.170\mu_B$, is in good agreement with the computational result, $3.171\mu_B$.

We measured the saturation magnetization $M(T)$ as a function of temperature over the range 5–350 K, as shown in Fig. 6. At low temperature, $T<70$ K, the magnetization curves follow the spin-wave theory with the functional form $M(T)=M(0)(1-AT^{3/2})$. Fitting the data to this form yields a best-fit value for $M(0)=72.21$ emu/g ($3.170\mu_B$), $A=3.71\times10^{-5}$ $K^{-3/2}$ (inset a). The spin-wave stiffness coefficient D from spin dispersion law $\hbar\omega=Dq^2$ may be calculated from the parameter A via the relation $A=2.612(V/S)\times(k_B/4\pi D)^{3/2}$, where V is the volume per magnetic atom and S is the spin. Calculation for Ni_2FeGa gives the value $D=90$ mev Å^2. Upon further heating the parent phase ($T>160$ K), M^2 becomes linear with T^2 (inset b). That is, $M(T)$ is expressed empirically as a function of temperature as $M(T)^2=M(0)^2(1-T^2/T_C^2)$. Linearly extrapolating to $T=0$ K, the spontaneous magnetization $M(0)$ can be determined as 69.76 emu/g ($3.035\mu_B$). It means that a less saturation magnetization would be expected if the Ni_2FeGa compound remained cubic structure at 0 K. By the same extrapolation to $M=0$ emu/g, the calculated Curie temperature of 430 K is in very good agreement with our previous experimental value measured by ac susceptibility.[6] The magnetization undergoes a change from $T^{3/2}$ to T^2 behavior and may come from the magnon-magnon interactions. The material undergoes a martensitic transformation, leading to the structural transition. The variation of magnetism arises from the change of dynamic interaction between magnons. Thus, we observed the magnetic behavior seems to evolve from Heisenberg-like at low temperature to itinerant magnetism at high temperature.[16] This kind of behavior was also observed in NiMnSb, in which Mn possesses localized magnetic moment. Differently, the mechanism for this crossover in NiMnSb, from spin-wave excitations to Stoner-like individual excitations, arises from the half-metallic ferromagnet to normal ferromagnet transition.[16]

In many Heusler alloys of Ni_2YZ, the ferromagnetism mainly contributes from the Y atoms. Among the Heusler alloys of Ni_2MnZ where the Mn atoms fully occupied the Y-fcc sites, many works indicated that an indirect d-d coupling achieved by conduction electrons makes the Mn atoms coupled as the ferromagnetic with a large magnetic moment ($3-4\mu_B$),[5] but the moment on Ni atoms is negligible. Our calculation shows that Ni_2FeGa is in the same case. When Ni_2FeGa structured in Heusler alloy, the nearest-neighbor Fe-Fe distance is about 4.05 Å, which is much larger than that in pure α-Fe and some other iron alloys, and ordinary direct coupling would have been insulated. Therefore, it is quite possible that the long-range magnetic coupling between localized moments through conducting electrons, which now is widely accepted as the dominant exchange mechanism in Mn-related Heusler alloys,[5] might also be valid in Fe-related Heusler alloys. Therefore, like Co_2FeZ alloys, the newly developed Heusler alloy Ni_2FeGa becomes one more good object to investigate the ferromagnetism of Fe in the indirect

coupling environment. Especially Ni_2FeGa exhibits martensitic transformation which has not been observed in other X_2FeZ Heusler alloys.

Furthermore, in order to compare the calculated value with the experimental value for iron moment in our Ni_2FeGa alloy, the moment of Ni, should be deducted from the total magnetic moment measured experimentally. In the present work, however, we could not measure the μ_{Ni} directly. Fortunately, there are many relevant results on it in the previous investigations.

Campbell reported that the contribution of Ni atom to the magnetization is zero in studying the magnetic properties of quartenary Heusler alloys $Ni_2Mn_xT_{1-x}Sn$ (T = Ti, V, Cr).[17] Buschow also reported a small μ_{Ni}, $0.065\mu_B$/f.u., in ternary Heusler alloy Ni_2CrAl.[18] In Heusler alloy Ni_2MnGa, although Webster did not give the exact value of Ni moment, they show clearly that polarized neutron measurements do suggest that there is a small Ni moment, less than $0.3\mu_B$.[19] All these results illustrate that the Ni atom provides a very little moment in Heusler alloy Ni_2YZ. Actually, it is evident from the DOS plot that the Ni $3d$ state has almost equal contributions in valence band for the majority and minority spins, as reported in X_2MnZ.[5]

More recently, however, the study of Brown *et al.* has indicated that the magnetization of Ni and Mn will be redistribution with the variation of temperature in Ni_2MnGa by means of polarized neutron scattering experiments.[15] The Ni moment is $0.24\mu_B$/atom and $0.36\mu_B$/atom for the parent and martensite phase, respectively. Furthermore, they have given a successful explanation by using band Jahn-Teller effect.

According to $\mu_{Ni}=0\mu_B$ suggested by Campbell and Buschow, the Fe moment has the largest value of about $3.170\mu_B$ in our Ni_2FeGa, that is, the ferromagnetism is totally from the Fe site. Following the estimation of $\mu_{Ni}=0.3\mu_B$ by Webster, however, iron moment still has a quite large value of $2.570\mu_B$/atom in Ni_2FeGa. Counting the redistribution of the Fe and Ni ferromagnetism upon the martensitic transformation as the work of Brown *et al.* work, taking the Ni moment of $0.360\mu_B$ at martensite phase (the largest reported value of Ni moment in Ni-based Heusler alloy up to now) and $0.24\mu_B$ for the austenite, the net moment value per iron atom is $2.450\mu_B$ for the martensite and $2.555\mu_B$ for the austenite. Thus, one can see that, in all experimental cases, the Fe moment in Ni_2FeGa is larger than that in pure α-Fe, $2.217\mu_B$/atom, by about 10–43 %.

We would like to evaluate here the utilization of the μ_{Ni} value. Taking $\mu_{Ni}=0$ might be possible in the case of some paramagnetic alloys, such as Ni_2CrAl, but not for the ferromagnetic compounds. Campbell *et al.* reported a doubtfully large value of $5\mu_B$/Fe atom in quaternary Heusler alloy $Ni_2Mn_{0.9}Fe_{0.1}Sn$ by neglecting the Ni moment (taking $\mu_{Ni}=0$).[20] On the other hand, taking the value from the martensite, $0.36\mu_B$,[15] seems to be so large that it would subsequently deduce a small value of Mn moment of about $3.40\mu_B$ in Ni_2MnGa, which is contrary to the fact of X_2MnZ Heusler alloys in which the Mn moment usually shows the nearly integral value of $4.0\mu_B$/atom. So far the consistent value of μ_{Ni} between calculation[11] and experiment[15] is $0.24\mu_B$/atom and is very close to our calculated value of $0.237\mu_B$ for the cubic and $0.271\mu_B$ for the orthorhombic.

Thus, our calculated μ_{Fe} value and the above experimental values all strongly suggested that Fe atom has a tendency to present a large magnetic moment in Ni_2FeGa. Clearly, such moment is larger than the value about $2.2\mu_B$ in Ni host and some other Fe-based alloys. Evidentially, in Heusler alloy X_2FeZ, such as Co_2FeGa and Co_2FeAl, the Fe moment is usually larger than $2.5\mu_B$;[21,22] it is $2.54\mu_B$ in semi-Heusler alloy PtFeSb;[23] and we reported similar results in quaternary NiMnFeGa Heusler alloys.[24]

Therefore, it is reasonable to believe that the large moment of Fe atom in Ni_2FeGa arises from the indirect coupling environment. It is very interesting to show some counterevidence that the iron moment would drop down to $2.2\mu_B$, once Fe atoms situate at the X site and have a direct coupling. For example, it occurred in the case of the investigation on the Fe moment as turning Co_2FeGa to Fe_2CoGa.[25,26]

Finally, for the Ni moment upon the martensite transition, let us turn back to the one we calculated. The calculation predicts that the Ni moment increased about 17% from 0.237 to $0.271\mu_B$ upon the martensitic transformation. This increased tendency has been experimentally observed in recent work of Brown *et al.* on NiMnGa alloy,[15] although there is a discrepancy between our calculation value and the experimental one.

In conclusion, the electronic structures of both the cubic and the orthorhombic are calculated in this paper. The results reveal that Fe atoms in Heusler alloy Ni_2FeGa tend to be behaved as localized moment like Mn in Heusler alloy X_2MnY. The DOS difference between the cubic and orthorhombic structures shows that a split of Ni peak near the Fermi level occurred through the structural transition, suggesting that a band Jahn-Teller effect is expected during this transformation. This transformation mechanism causes the redistribution of electron, leading to the increase of Ni magnetization. The computational saturation magnetic moment of the martensite for Ni_2FeGa is $3.171\mu_B$, very close to the experimental value, $3.170\mu_B$. It has been analyzed that Fe atoms contributed a moment up to $2.450–3.170\mu_B$ to the Ni_2FeGa compound based on the different possible values of Ni moment in Heusler alloys shown in references, which is about 10–43 % larger than that of pure Fe. This large moment behavior arises from the indirect interaction between Fe-Fe atoms through conduction electrons. We also find that temperature dependence of saturation magnetization shows evidence of spin-wave excitations at low temperature and Stone excitations at high temperatures, which may be due to the change of interaction between magnon arising from martensitic transformation.

The authors would like to appreciate Professor Dingsheng Wang for his helpful discussion on the electronic structure calculation. This work was supported by National Natural Science Foundation of China Grant No. 50131010.

*Author to whom correspondence should be addressed. Electronic address: userm201@aphy.iphy.ac.cn

[1] F. Heusler, W. Starck and E. Haupt, Verh. Dtsch. Phys. Ges. **5**, 220 (1903).
[2] P.J. Webster and R.S. Tebble, J. Appl. Phys. **39**, 471 (1968).
[3] G. Malmstrom, D.J.W. Geldart, and C. Blomberg, J. Phys. F: Met. Phys. **6**, 1953 (1976).
[4] S. Ishida, S. Sugimura, S. Fujii, and S. Asana, J. Phys.: Condens. Matter **3**, 5793 (1991).
[5] J. Kübler, A.R. Williams, and C.B. Sommers, Phys. Rev. B **28**, 1745 (1983).
[6] Z.H. Liu, M. Zhang, Y.T. Cui, Y.Q. Zhou, W.H. Wang, G.H. Wu, X.X. Zhang, and G. Xiao, Appl. Phys. Lett. **82**, 424 (2003).
[7] K. Oikawa, T. Ota, T. Ohmori, Y. Tanaka, H. Morito, A. Fujita, R. Kainuma, K. Fukamichi, and K. Ishida, Appl. Phys. Lett. **81**, 5201 (2002).
[8] E. Wimmer, H. Krakauer, M. Weinert, and A.J. Freeman, Phys. Rev. B **24**, 864 (1981).
[9] M. Weinert, E. Wimmer, and A. J. Freeman, Phys. Rev. B **26**, 4571 (1982).
[10] J. Rath and A.J. Freeman, Phys. Rev. B **11**, 2109 (1975).
[11] S. Fujii, S. Ishida, and S. Asano, J. Phys. Soc. Jpn. **58**, 3657 (1988).
[12] J. Yamashita, S. Asano, and S. Wakoh, Prog. Theor. Phys. **47**, 774 (1972).
[13] M. Zhang and G. H. Wu (unpublished).
[14] M. Zhang, Z.H. Liu, and G.H. Wu, Solid State Commun. **128**, 107 (2003).
[15] P.J. Brown, A.Y. Bargawi, J. Crangle, K.U. Neumann, and K.R.A. Ziebeck, J. Phys.: Condens. Matter **11**, 4715 (1999).
[16] C. Hordequin, J. Pierre, and R. Currat, J. Magn. Magn. Mater. **162**, 75 (1984).
[17] C.C.M. Campbell, J. Magn. Magn. Mater. **3**, 354 (1976).
[18] K.H.J. Buschow and P.G. van Engen, J. Magn. Magn. Mater. **25**, 90 (1981).
[19] P.J. Webster, K.R.A. Ziebeck, S.L. Town, and M.S. Peak, Philos. Mag. B **49**, 295 (1984).
[20] C.C.M. Campbell and J.A. Cameron, J. Phys. F: Met. Phys. **8**, 1591 (1978).
[21] P.J. Brown, K.U. Neumann, P.J. Webster, and K.R.A. Ziebeck, J. Phys.: Condens. Matter **12**, 1827 (2000).
[22] I. Galanakis, P.H. Dederichs, and N. Papanikolaou, Phys. Rev. B **66**, 174429 (2002).
[23] K.H.J. Buschow, J.H.N. van Vucht, P.G. van Engen, D.B. de Mooij, and A.M. van der Kraan, Phys. Status Solidi A **75**, 617 (1983).
[24] Z.H. Liu, M. Zhang, W.Q. Wang, W.H. Wang, J.L. Chen, G.H. Wu, F.B. Meng, B.D. Liu, H.Y. Liu, J.P. Qu, and Y.X. Li, J. Appl. Phys. **92**, 5006 (2002).
[25] A. Ayuela, J. Enkovaara, K. Ullakko, and R.M. Nieminen, J. Phys.: Condens. Matter **11**, 2017 (1999).
[26] A. Deb, M. Itou, Y. Sakurai, N. Hiraoka, and N. Sakai, Phys. Rev. B **63**, 064409 (2001).